9 T high magnetic field annealing effects on FeN bulk sample

Yanfeng Jiang, Vivekanand Dabade, Michael P. Brady, Orlando Rios, Richard D. James, and Jian-Ping Wang

Articles you may be interested in

Strain effect of multilayer FeN structure on GaAs substrate
J. Appl. Phys. **113**, 17E149 (2013); 10.1063/1.4800086

Epitaxial high saturation magnetization FeN thin films on Fe(001) seeded GaAs(001) single crystal wafer using facing target sputterings
J. Appl. Phys. **109**, 07B767 (2011); 10.1063/1.3565403

Effect of high magnetic fields on the morphology of soft magnetic - FeN films
J. Appl. Phys. **93**, 9145 (2003); 10.1063/1.1570505

Annealing study of Fe 2 O 3 nanoparticles: Magnetic size effects and phase transformations
J. Appl. Phys. **91**, 4611 (2002); 10.1063/1.1457544

The effect of oxygen on magnetic properties and corrosion resistance of Fe–N thin films
J. Appl. Phys. **85**, 4571 (1999); 10.1063/1.370411

9 T high magnetic field annealing effects on FeN bulk sample

Yanfeng Jiang,[1] Vivekanand Dabade,[2] Michael P. Brady,[3] Orlando Rios,[3] Richard D. James,[2] and Jian-Ping Wang[1,a)]

[1]*Department of Electrical and Computer Engineering, University of Minnesota, Minneapolis, Minneota 55455, USA*
[2]*Department of Aerospace Engineering and Mechanics, University of Minnesota, Minneapolis, Minnesota 55455, USA*
[3]*Materials Science and Technology Division, Oak Ridge National Laboratory, Oak Ridge, Tennessee 37831–6115, USA*

α''-$Fe_{16}N_2$ has been suggested as a promising candidate for future rare-earth-free magnets. In this paper, we report to use high magnetic field (9 T) assisted post-annealing process to enhance the $Fe_{16}N_2$ phase formation in FeN bulk rod samples during the $\alpha' \rightarrow \alpha''$ phase transformation and thus improve its magnetic properties. It was found by X-ray Diffraction measurement that the volume ratio of $Fe_{16}N_2$ phase was increased up to 22%, which corresponds to an increase in the amount of transformation from $\alpha' \rightarrow \alpha''$ up to 78%. Also, the saturation magnetization (M_s) of the prepared FeN rod sample was increased to 227 emu/g with its coercivity up to 376 Oe at room temperature. A working mechanism for the high field assisted post-annealing process was presented. © 2014 AIP Publishing LLC. [http://dx.doi.org/10.1063/1.4868493]

I. INTRODUCTION

Permanent magnets can provide high efficiency and reliability for renewable energy technologies, including electrical vehicles and wind turbines.[1,2] Because rare earth permanent magnets have supply constraints and high price,[3] a new magnet with more abundant and less strategically important elements is desired to replace rare earth magnets. One of the most promising candidates is α''-$Fe_{16}N_2$ because of its giant saturation magnetization and large magnetocrystalline anisotropy.[1,4]

α''-$Fe_{16}N_2$ phase was first discovered by Jack,[5] but its magnetic properties remained unexplored until 1972 when Kim and Takahashi[6] reported its high magnetization in films, which was obtained by evaporating iron onto a glass substrate in low-pressure nitrogen. This discovery has inspired many groups all over the world to explore the material by using different preparation methods. These include thin films grown by molecular beam epitaxy (MBE),[7,8] facing target sputtering,[9–11] reactive magnetron sputtering,[12,13] ion implantation,[14–16] and ion beam deposition.[17,18] The experimental results were inconsistent and no conclusions were made since 1999. Recently, we reported to synthesize $Fe_{16}N_2$ thin films with giant saturation magnetization and the support of a proposed cluster+atom model and experimental evidence of partially localized 3d electron.[4]

Encouraged by the promising magnetic properties demonstrated by thin films, researchers have been investigating how to prepare bulk samples with larger volume fraction of $Fe_{16}N_2$ phase while exhibiting the same promising magnetic properties. A bottom-up approach has been the main stream in preparation of bulk samples[18–20] in which iron powder or foil was used as starting materials since samples of this size

would be easier to nitride. Those experiments have followed essentially Jack's early approach[5] via γ and α' in which the nitrogen austenite was prepared by heating powders or foils in atmosphere by flowing NH_3/H_2 over 700 °C for several hours. The sample was then quenched to room temperature or in liquid nitrogen. During this process, the γ phase partially transforms into the α' phase through the fcc to bct (martensitic) transformation. Heat treatment at 120 °C orders interstitial nitrogen atoms in the α' phase and then α'' phase precipitates are formed. Huang et al.[19] claimed 56% α'' phase with a large saturation magnetization (4πMs) 2.65 ± 0.15 T, corresponding to 2.95 ± 0.15 μB per Fe atom, a 34% increase over that of α-Fe. Coey et al.[20] produced the sample with 40% α'' phase, with a saturation magnetization value of 2.3 ± 0.2 T, which is only about 10% higher than that of α-Fe but are in broad agreement with the band-structure calculations. Bao et al.[21] started from hydrogen-reduced Fe_2O_3 and convert up to 30% FeN into α'' phase.

We proposed a different approach to synthesize bulk FeN sample starting with bulk iron; herein, it is called a top-down method. The detailed information can be found at Ref. 22. Starting from the as-prepared FeN bulk rod, the effect of high magnetic field (9 T) post-annealing on the phase transformation and magnetic properties of FeN bulk samples were investigated in this paper.

Four different phases and three phase transformations were involved to synthesize the α''-$Fe_{16}N_2$ phase, namely, $\alpha \rightarrow \gamma \rightarrow \alpha' \rightarrow \alpha''$.[5] Until now, the published works have been focused on the $\gamma \rightarrow \alpha'$ martensitic transformation stage by using an external magnetic fields.[22,23] Kakeshita et al.[23] have carried out systematic studies which involved the effects of an external magnetic field on the kinetics of martensitic transformation and confirmed that the magnetic field could assist the phase transformation. Koyano et al.[24] have used the magnetic field to increase the fraction of the α'

a)Author to whom correspondence should be addressed. Electronic mail: jpwang@umn.edu.

phase transformed from the γ phase. They found an external magnetic field could assist the $\gamma \rightarrow \alpha'$ martensitic transformation. So far, there is no report on the effects of external magnetic field on the $\alpha' \rightarrow \alpha''$ phase transformation. Furthermore, there is also no report on the effects of high magnetic field (9 T) for FeN bulk materials. Here, the effects of high magnetic field (9 T) annealing on the $\alpha' \rightarrow \alpha''$ phase transformation were investigated.

II. EXPERIMENTAL PROCEDURE

The technical approach to prepare the FeN rod was described in Ref. 22. The size of the FeN samples prepared for the high magnetic field post-annealing is 10 mm in length, square cross section with 1 mm side length. The high field annealing experiment was conducted at Oak Ridge National Laboratory. After the bulk pure iron was mixed with nitrogen and cut into the FeN bulk rod,[22] it was water quenched and cooled at liquid nitrogen temperature for 20 h to aid the FeN transformation from austenite phase into martensite phase. Then, a post-annealing process at 150 °C with 9 T magnetic field was conducted for 20 h. Magnetic field was applied in parallel with the wire's length direction (in-plane orientation) in order to minimize the eddy current and the demagnetization factor. For comparison, another sample prepared by the same procedure but without applying high field during the post-annealing was used as reference to study the effects of high magnetic field.

Magnetization curves were measured at room temperature using a superconducting quantum interference device (SQUID) magnetometer (Quantum Design MPMS-XP) in a magnetic field of $-2\,\mathrm{T} \leq \mathrm{B} \leq +2\,\mathrm{T}$.

III. RESULTS AND DISCUSSION

The X-ray Diffraction (XRD) spectra of the FeN rod samples before and after quenching are shown in Fig. 1. X-ray test configuration was that the incident X-ray is perpendicular to the rod's side plane. The strongest diffraction line is (110), which implies that the FeN bulk sample might possess (110) preferred texture orientation. Before the quenching process, the sample is a solid mixture of Fe and N so that the main phase is Fe. There appeared a small peak of $Fe_4N(200)$, as shown in Fig. 1, which could be generated during FeN rod preparation.[22]

As shown in Fig. 1, the Fe_8N phase appeared after quenching, with 28% volume ratio calculated with $Fe_8N(202)$ peak. Additionally, the oxide line $Fe_3O_4(121)$ also appeared with 6%, which could come from the preparation stage. The Fe volume ratio was estimated to be 54% and the rest ($\sim$12%) is Fe_4N. Therefore, after quenching, the sample turns out to be a mixture of bcc and bct phases.

Based on the standard diffraction intensity data of a powder sample without any orientation, the ratio of diffraction intensities between $Fe_8N(202)$ and $Fe_8N(112)$ peak should be 100:1. However, by integrating the peaks of $Fe_8N(202)$ and $Fe_8N(112)$, the ratio of actual areas between these two peaks is about 1:1.5. This means the diffraction intensity of $Fe_8N(112)$ peak was much stronger than that of powder ones. At the same time, the observed ratio between $Fe_8N(202)$ and $Fe_8N(002)$ is almost as same as the powder's

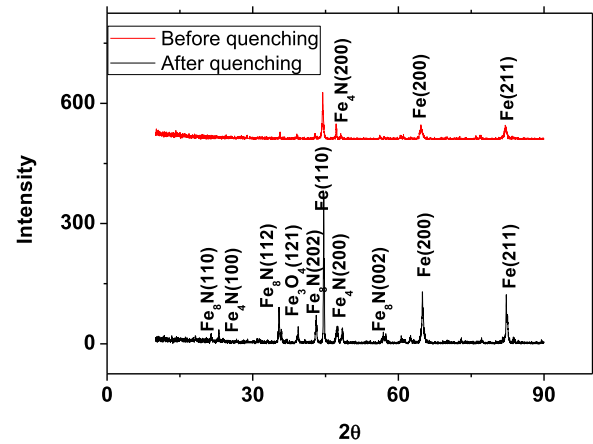FIG. 1. X-ray diffraction spectra for sample before and after quenching. Before quenching, the main phase is α-Fe, with a small peak of Fe_4N. After quenching, the sample turns out to be a mixture of bcc and bct phases.

value. This indicates that the diffraction intensity from b axis was enhanced. Since the x-ray is perpendicularly injected into sample's side plane, the b axis lies vertically to the sample plane while a and c axis lie in the sample plane.

Figure 2 shows the XRD spectra after annealing. For comparison, results with and without high field are listed together in this figure. It is clear that high field post-annealing modified the phase constitution and crystalline orientation of the FeN sample. The $Fe_{16}N_2$ volume ratio was increased as evidenced by the increase of the $Fe_{16}N_2$ (002) and (004) peaks intensity.

A comparison has been made for the FeN rod samples post-annealing with and without applying high magnetic field as listed in Table I.

Table I shows that the volume ratios of Fe, Fe_4N, and Fe_3O_4 remain the same with and without high field. However, the volume ratio of α'' phase for the sample post-annealed with high field is higher than that by normal annealing (w/o high field). The increment of α'' phase should come from the α' phase. The total volume ratio of α' is 28% after quenching. For the sample after normal post-annealing, there are 18%
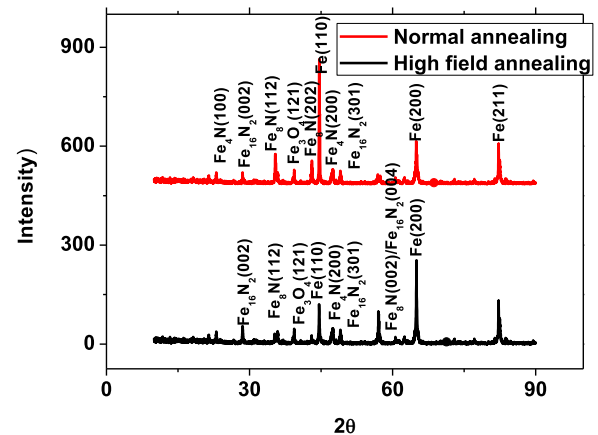

FIG. 2. X-ray diffraction spectra for samples with and without high field assistance. The volume ratios of Fe, Fe_4N, and Fe_3O_4 remain the same at the two annealing conditions. The volume ratio of α'' phase after high field annealing is higher than that by normal annealing. For the normal annealing, only 35% of Fe_8N has transformed into α'' phase. For the sample after a high field annealing, there are 6% Fe_8N and 22% $Fe_{16}N_2$, respectively, corresponding to 78% transformation from α' phase.

TABLE I. Comparison of volume ratios by normal and high field annealing.

	Volume ratio (normal annealing)	Volume ratio (high field annealing)
Fe	54%	54%
$Fe_{16}N_2$	10%	22%
Fe_8N	18%	6%
Fe_4N	12%	12%
Fe_2O_3	6%	6%

Fe_8N and 10% $Fe_{16}N_2$ phase, respectively. This means only 35% of Fe_8N has transformed into α'' phase. On the other hand, for the sample after a high field annealing, there are 6% Fe_8N and 22% $Fe_{16}N_2$, respectively, corresponding to 78% transformation from α' phase. This demonstrates that high magnetic field assistance during the post-annealing does promote the phase transformation rate from Fe_8N to $Fe_{16}N_2$.

Considering the difference of peak intensities between the two spectra in Fig. 2, there are three scenarios, namely, intensity enhancement, intensity decrement, and no difference, as listed in Table II.

Based on magnetic properties measured by SQUID, the saturation magnetization (M_s) of the high field annealed sample was increased to 227 emu/g with the coercivity up to 376 Oe at room temperature.

Here, we experimentally verified that 9 T magnetic field does improve the magnetic properties of bulk FeN rod sample by modifying the phase constitution and crystalline orientation. The transforming rate from α' was increased to 78%. In terms of transformation process $\alpha \rightarrow \gamma \rightarrow \alpha' \rightarrow \alpha''$, the final percentage of α'' should depend on the transforming rate of $\gamma \rightarrow \alpha'$ and $\alpha' \rightarrow \alpha''$. Koyano *et al.*[24] have demonstrated that high field can improve the rate of $\gamma \rightarrow \alpha'$ up to 92%. Here, for the first time, we show that the transforming percentage of $\alpha' \rightarrow \alpha''$ can reach 78%. So, based on the two stages' phase transformation results, it is anticipated that the ideal percentage of α'' phase should be 72% if high magnetic field is applied during both phase transformations processes.

The mechanism of the high field effects on the $Fe_{16}N_2$ phase formation could be understood based on the free energy argument. At the beginning, for α' phase, nitrogen atoms are arranged in a disordered manner on octahedral sites along the c axis. Its phase transformation into α'' corresponds to nitrogen reassembled in an ordered way. However, the transformation cannot occur easily because of the strain effect.[25] Here, the strain effect means a strain energy accumulation inside the sample, which can suppress any further progress of the phase

transformation. For the FeN rod material, the main contribution of strain energy accumulation comes from the quenching stage since the martensitic transformation from fcc to bct accompanies atomic volume increase. This accumulation will hinder the following $\alpha' \rightarrow \alpha''$ transformation. In fact, the transforming rate from $\alpha' \rightarrow \alpha''$ under any previously reported normal annealing process was only 35%.

The direction of the strain effect is related to the matrix orientation. As shown in Fig. 1, the main matrix orientation is (110). Based on the analysis of a relative intensities of different peaks, it indicates that the b axis lies out of the sample plane while the a and c axis lie in the sample plane. That means the in-plane 9 T field is perpendicular to the b axis. This could account for the decrease of Fe(110) intensity and increase of Fe(200), as shown in Fig. 2. Based on the above analysis, high field in the plane can degenerate the strain effect; and therefore, increase the $\alpha' \rightarrow \alpha''$ transforming rate. Since the magnetic field is aligned with the FeN (002) orientation, Gibbs free energy on the prolonged c axis is decreased and thus is helpful for $Fe_{16}N_2$ (004) and $Fe_{16}N_2$ (002) phase transformation.

IV. CONCLUSION

The effects of high magnetic field (9 T) post-annealing process on the $\alpha' \rightarrow \alpha''$ transformation ($Fe_8N \rightarrow Fe_{16}N_2$) for FeN bulk rod samples were investigated. It shows that high field annealing modifies the phase constitution and crystalline orientation of the FeN rod sample. The amount of transformation from $\alpha' \rightarrow \alpha''$ increased to 78%. The saturation magnetization (M_s) of the rod sample with a high field annealing was increased to 227 emu/g with the coercivity up to 376 Oe at room temperature.

TABLE II. Relative changes in peak intensities after the high field annealing, compared with the normal annealing result.

Phase (intensity decreased after high field annealing)	Phase (intensity enhanced after high field annealing)	Phase (without difference)
Fe(110)	Fe(200)	Fe(211)
$Fe_8N(112)$	$Fe_{16}N_2(004)$/$Fe_8N(002)$	$Fe_{16}N_2(301)$
$Fe_8N(202)$	$Fe_{16}N_2(002)$	$Fe_4N(200)$
		$Fe_3O_4(121)$
		$Fe_4N(100)$

[1] S. Chu and A. Majumdar, Nature **488**, 294 (2012).
[2] J. M. D. Coey, J. Magn. Magn. Mater. **248**, 441 (2002).
[3] L. H. Lewis and F. Jimenez-Villacorta, Metall. Mater. Trans. A **44A**, 2 (2013).
[4] J.-P. Wang *et al.*, IEEE Trans. Magn. **48**, 1710 (2012).
[5] K. H. Jack, Proc. R. Soc. London, Ser. A **208**, 200 (1951).
[6] T. K. Kim and M. Takahashi, Appl. Phys. Lett. **20**, 492 (1972).
[7] Y. Sugita *et al.*, J. Appl. Phys. **76**, 6637 (1994).
[8] Y. Sugita *et al.*, J. Appl. Phys. **79**, 5576 (1996).
[9] N. Ji *et al.*, Phys. Rev. B. **84**, 245310 (2011).
[10] D. C. Sun *et al.*, J. Appl. Phys. **79**, 5440 (1996).
[11] N. Ji *et al.*, Appl. Phys. Lett. **98**, 092506 (2011).
[12] H. Takahashi *et al.*, J. Magn. Magn. Mater. **174**, 57 (1997).
[13] M. A. Brewer *et al.*, J. Appl. Phys. **81**, 4128 (1997).
[14] H. Shinno and K. Saito, Surf. Coat. Technol. **103–104**, 129 (1998).
[15] K. Nakajima and S. Okamoto, Appl. Phys. Lett. **54**, 2536 (1989).
[16] T. Weber *et al.*, Thin Solid Films **279**, 216 (1996).
[17] S. Okamoto *et al.*, J. Appl. Phys. **79**, 5250 (1996).
[18] Z. Y. Yao *et al.*, J. Magn. Magn. Mater. **177–181**, 1291 (1998).
[19] M. Q. Huang *et al.*, J. Magn. Magn. Mater. **135**, 226 (1994).
[20] J. M. D. Coey, J. Appl. Phys. **76**, 6632 (1994).
[21] X. Bao *et al.*, J. Appl. Phys. **75**, 5870 (1994).
[22] J.-P. Wang *et al.*, "Iron nitride permanent magnet and technique for forming iron nitride permanent magnet," U.S. patent pending (21 February 2013).
[23] T. Kakeshita *et al.*, Mater. Trans. JIM **34**, 415 (1993).
[24] T. Koyano *et al.*, J. Appl. Phys. **100**, 033906 (2006).
[25] N. Ji *et al.*, Appl. Phys. Lett. **102**, 072411 (2013).